Appl. Phys. B 92, 247–252 (2008)
DOI: 10.1007/s00340-008-3074-7

Applied Physics B
Lasers and Optics

P.P. SAHU

Polarization insensitive thermally tunable add/drop multiplexer using cascaded Mach–Zehnder coupler

Department of Electronics and Communication Engineering, Tezpur University, Tezpur 784028, Assam, India

Received: 24 September 2007/Revised version: 8 April 2008
Published online: 20 June 2008 •

ABSTRACT In this paper, a thermally tunable add/drop multiplexer based on a *Y* symmetric cascaded Mach–Zehnder (CMZ) coupler is found to be polarization dependent due to the stress anisotropy caused by local heating to achieve thermooptic phase change. A thermooptic delay line structure with a stress releasing groove is proposed for reduction of the polarization dependence of a *Y* symmetric delay line coupler of high index contrast waveguides. It is seen that thermally tunable transmission characteristics of a *Y* symmetric CMZ device based on the proposed structure is almost polarization independent. It is also found that the reduction of the heating power in the proposed structure is ~ 1.6 times smaller than that of the conventional structure.

PACS 29.27.Fh; 52.38.Kd

1 Introduction

In optical networks, an add/drop multiplexer is one of the key components that adds/drops one or more wavelengths by thermal tuning via the thermooptic effect. The add/drop multiplexers using 2×2 cascaded Mach–Zehnder (CMZ) filters [1–6] are particularly interesting because of their simplicity of configuration and ease of fabrication in comparison to other types of filters, such as Bragg grating assisted reflected filters [7, 8], and Meander coupler type filters [9]. To accommodate a larger number of channels in add/drop multiplexing, *Y* symmetry cascaded Mach–Zehnder (CMZ) filters have been previously used [1–6], due to their low pass band width. The use of high index contrast waveguides, which are strongly guided, makes the device shorter. In this paper, SiO_2/silicon oxinitride (SiON) material has been used due to the availability of high index contrast, compatibility with conventional silicon based IC processing, polarization insensitiveness, high stability, etc. We have already studied [10] different stages of a *Y* symmetry CMZ filter with different coupler distribution to obtain more channels with crosstalk ≤ -25 dB, which is normally required to avoid cumulative propagating losses. For thermal tuning of the filter, many thermooptic structures have been reported [11, 12]. A bridge-suspended structure has been used previously [11] for lower heating power resulting in longer response time. We have proposed and studied the thermooptic device with a silicon trench below the heater for reduction of heating power [12], but in these structures, polarization dependence is not considered. On the other hand, the thermooptic phase shifting device was found to exhibit polarization dependence of about 3.1% between TE and TM modes [13]. The main contribution that led to the polarization dependence of thermal tuning due to local heating by a thin film heater are temperature gradients and thermal expansion coefficients of the materials [14]. Offrein et al. [14] has demonstrated different materials for the reduction of polarization dependence by considering thermal expansion and the width of the heater. In this paper the temperature gradients are considered for study of the stress release groove in which, higher is the magnitude of temperature gradients, more is the stress release.

In this paper, polarization dependent characteristics of an add/drop multiplexer based on a *Y* symmetric cascaded Mach–Zehnder coupler is presented. A thermooptic delay line structure is proposed for reduction of polarization dependence. It is found from temperature profiles that temperature gradients of the proposed structure which mainly cause the release of stress anisotropy are more than that of conventional structures. Finally, polarization independent transmission characteristics of a CMZ coupler based on the proposed structure is also shown.

2 Polarization dependent characteristics of *Y* symmetric CMZ filter

A rigorous review of the theory and applications of CMZ filters consisting of delay lines (MZ coupler with unequal arms) has been provided by different authors [3, 10, 15] in which a *Y* symmetry CMZ filter is preferred for add/drop fliter application, because of their lower pass band in comparison to point symmetry CMZ couplers [16]. Figure 1 shows a $2 \times 2N$ stage *Y* symmetry cascaded Mach–Zehnder coupler consisting of N delay line sections with arm lengths L_A and L_B (where the path difference between two arms is $\Delta L = L_A - L_B$), thin film heater of length L_H ($L_H \approx L_A$) and width W_H made on a curved arm of the MZ section, and $N+1$ two mode interference (TMI) couplers of width $2w$ (where

✉ Fax: +91-03712-267006, E-mail: pps@tezu.ernet.in

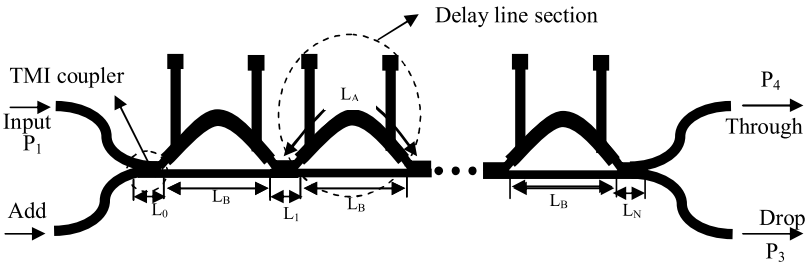

FIGURE 1 *N*-stage *Y* symmentric CMZ circuit using TMI coupler and thin film heater

w = width of a single mode access waveguide). The core and cladding are chosen to be SiON and SiO_2, respectively, due to the availability of wide index contrast, compatibility with conventional silicon based IC processing, high stability, etc. In the figure, the couplers of the device are assumed to act as one long coupler with total coupling length L, which are distributed in different ways over all individual couplers of the circuit, where $L = \sum_{k=0}^{N} L_i$ and L_i is the length of ith coupler ($i = 0, 2, 3, ..., N$). The coupling length distribution which controls transmission characteristics of the filter is discussed later. Each TMI coupler consists of a two mode coupling region in which only fundamental and first order modes with propagation constants β_{00} and β_{01}, respectively, are excited in the coupling region [17] and the coupling coefficient (k_T) of the TMI coupler is represented by $(\beta_{00} - \beta_{01})/2$. From the geometry of the figure, the length of each delay line section is obtained as $L_B \approx H^2/\Delta L$, where H is the height of the delay line section. The refractive indices of the core and its surrounding cladding are n_1 and n_2, respectively. The input power P_1 is incident on the lowest waveguide when the output powers P_3 and P_4 are obtained as a cross state and bar state, respectively. The normalized cross power of the N-stage Y symmetric cascaded Mach–Zehnder coupler is given by

$$\frac{P_3}{P_1} = \left\{ \sum_{k=0}^{N} |a_k|^2 + 2 \sum_{i=0}^{N} a_i \sum_{k=i+1}^{N} a_k \times \cos[(k-i)\Delta\varphi(\lambda, \Delta L, P)] \right\} e^{-N\alpha L_B}, \quad (1)$$

where, α is the bending loss coefficient depending on bending radius [10, 18]. The coefficients a_k of the normalized cross state power are determined from the coupling coefficient k_T of TMI couplers [10, 17]. The term $\Delta\varphi(\lambda, \Delta L, P)$ is the phase difference introduced by the length difference between two arms of the delay line section plus the phase shift introduced by the heating curved arm with heating power P. Expanding to first order in wavelength, $\Delta\varphi(\lambda, \Delta L, P)$ can be written as

$$\Delta\varphi(\lambda, \Delta L, P) = 2\pi[\varphi(\Delta L) + \varphi(P)] \left\{ 1 - \frac{\lambda - \lambda_{\text{ref}}}{\lambda_{\text{ref}}} \right\}, \quad (2)$$

where, $\varphi(\Delta L) = \frac{n_{\text{eff}} \Delta L}{\lambda}$, n_{eff} is effective index at wavelength λ, and λ_{ref} is the reference wavelength. When the waveguide is heated locally via the heater, the glass (SiO_2) can expand freely to the Si substrate, but it can not expand freely in the parallel direction, because it is surrounded by the other glass (SiO_2). So, a compressive stress occurs only in the parallel direction and it mainly induces an increase in refractive index in the TM mode. In the case of the TM mode $\varphi(P)$, a phase change due to application of heating power P occurs not only due to the isotropic thermooptic phase $\varphi_T(P)$ ($\varphi_T(P) = \frac{dn}{dT} \Delta T_c(P) \frac{L_H}{\lambda}$, where, $\frac{dn}{dT}$ = thermooptic index coefficient, $\Delta T_c(P)$ is temperature difference between two cores), but also due to an anisotropic stress optic phase $\varphi_S(P)$. The anisotropic stress optic phase change for the temperature difference $\Delta T_c(P)$ between two cores obtained by heating via a heater is expressed as

$$\varphi_S(P) = \frac{d(n_{TM} - n_{TE})}{dT} \Delta T_c(P) \frac{L_H}{\lambda}, \quad (3)$$

where $\frac{d(n_{TM} - n_{TE})}{dT}$, the temperature rate of increase of birefringence depending on stress optical coefficient $\frac{\delta(n_{TM} - n_{TE})}{\delta S}$, Young's modulus $\frac{\delta S}{\delta V}$ and the thermal expansion coefficient $\frac{\delta V}{\delta T}$ are expressed as

$$\frac{d(n_{TM} - n_{TE})}{dT} = \frac{\partial(n_{TM} - n_{TE})}{\partial S} \frac{\partial S}{\partial V} \frac{\partial V}{\partial T}. \quad (4)$$

In the case of the TE mode, the phase change with the application of heating power $\varphi(P)$ is only an isotropic phase change, $\varphi_T(P)$.

We have already studied [10] different stages of a Y symmetric CMZ coupler with different coupler distributions

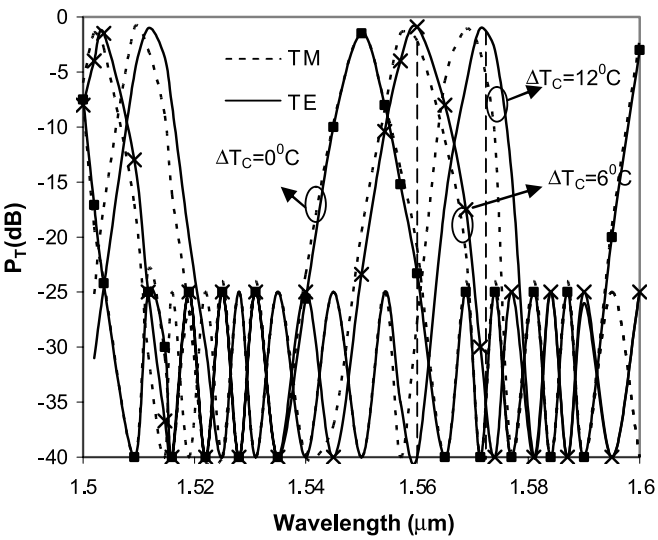

FIGURE 2 Polarization dependent thermally tunable normalized cross state power of two-stage Y symmetric CMZ filter based on conventional thermooptic delay line structure with $\Delta n = 5\%$ $\lambda_{\text{ref}} = 1.55\,\mu\text{m}$, cladding index = 1.447, waveguide core width $w = 1.5\,\mu\text{m}$, $\Delta L = 20.5\,\mu\text{m}$ and $L_B = 462\,\mu\text{m}$ (the *dashed straight line* is used for indicating cross state power in dB for TE polarization)

in which a five-stage CMZ coupler with truncated binomial coupler distribution (truncated parameters $M = 7$ and $r = 2$, $N =$ number stages $= M - 2r$) using $\Delta n = 5\%$, and waveguide core width $w = 1.5\,\mu$m, provides 37 channels for a 100 GHz channel spacing with crosstalk of ~ -25 dB. Figure 2 shows simulation results of thermally tunable polarization dependent cross state transmission characteristics obtained by using (1)–(4) for a five-stage Y symmetric CMZ circuit using waveguide core of SiON and cladding of SiO_2 with $\Delta n = 5\%$, $\lambda_{\text{ref}} = 1.55\,\mu$m, $\Delta L = 10.5\,\mu$m, $L_B = 462\,\mu$m and $w = 1.5\,\mu$m. In the figure the dashed line represents the normalized cross state power (P_3/P_1) of TM polarization obtained by using (1)–(4) and the dispersion equation [19], which is required for calculation of the propagation constant for TM polarization. The solid line indicates the normalized cross state power (P_3/P_1) of TE polarization obtained by using (1)–(4) and the dispersion equation [19] of TE polarization. It is seen that the peak cross state normalized power of TE and TM polarization is obtained at almost the same resonant wavelength of 1.55 μm (wavelength satisfying phase change of $2\pi n$ where, n is an integer), which is completely transmitted in cross state without application of heating power. With application of heating power by a heater, the temperature difference $\Delta T_c(P)$ between the cores of waveguide arms for the delay line section is achieved. It is seen from the figure that for the temperature difference, $\Delta T_c(P)$ of 6 and 12 °C, the shifted resonant wavelengths for TM polarizations are ~ 1.5572 and $\sim 1.568\,\mu$m, respectively, and for TE polarization, they are ~ 1.56 and $\sim 1.571\,\mu$m, respectively. The difference between resonant wavelength shifts for TE and TM polarizations is due to the extra phase difference obtained with the application of heating power for TM polarization in comparison to TE polarization, due to the anisotropic stress optic effect as discussed earlier. This polarization dependence of cross state transmission curves provides polarization dependent loss (PDL) which is expressed as

$$\text{PDL} = -10\log_{10}\left(\frac{P^{\text{TM}}}{P^{\text{TE}}_{\text{max}}}\right), \tag{5}$$

where $P^{\text{TE}}_{\text{max}}$ is the peak normalized cross state power of TE polarization at the resonant wavelength, and P^{TM} is the normalized cross state power of TM polarization at the same resonant wavelength, as shown in Fig. 2 by the dashed straight line. The PDL of the device estimated from the figure for $\Delta T_c(P)$ of 6 and 12 °C are ~ 0.9 and ~ 1.8 dB, respectively. The PDL increases with increase of $\Delta T_c(P)$. Apart from the polarization dependent loss, other loss is radiation loss in the bending portion of the delay lines of the device. But in all cases, the height of the side lobes (treated as a crosstalk) and filtered width of transmission characteristics remains almost same.

3 Proposed thermooptic delay line structure

Based on the above polarization dependent characteristics and considering reduction of polarization dependence, a thermooptic delay line structure is proposed as shown in Fig. 3. The structure has four sides or boundaries: top surface (side A), bottom surface (side B), left side surface (side C) and right surface (side D). We have already studied [12] thermal analysis of conventional and low power thermooptic device structures with a silicon trench at the bottom surface and optimized device parameters such as heater width, total cladding width, trench width, etc. Like these structures, the proposed delay line structure has two waveguides, with an addition of a groove of width W_G and depth H_G made in between two waveguide cores at its top surface for the release of stress anisotropy, which induces mainly a refractive index increase in the TM polarization [13]. It contains air medium where the temperature is considered to be the ambient temperature, which is slightly higher than room temperature T_I. The bottom and right side surfaces of the silicon trench, made just below the heater in the proposed structure, are attached to the substrate whereas the left side surface of the trench is attached to the heat insulator. The position of the waveguide cores and their sizes, heater size and position, upper cladding thickness W_{oc} and total cladding thickness W_c, trench width and thickness are kept the same as those of the conventional structure. Both side surfaces of the proposed structure are assumed as heat insulator for suppressing lateral heat diffu-

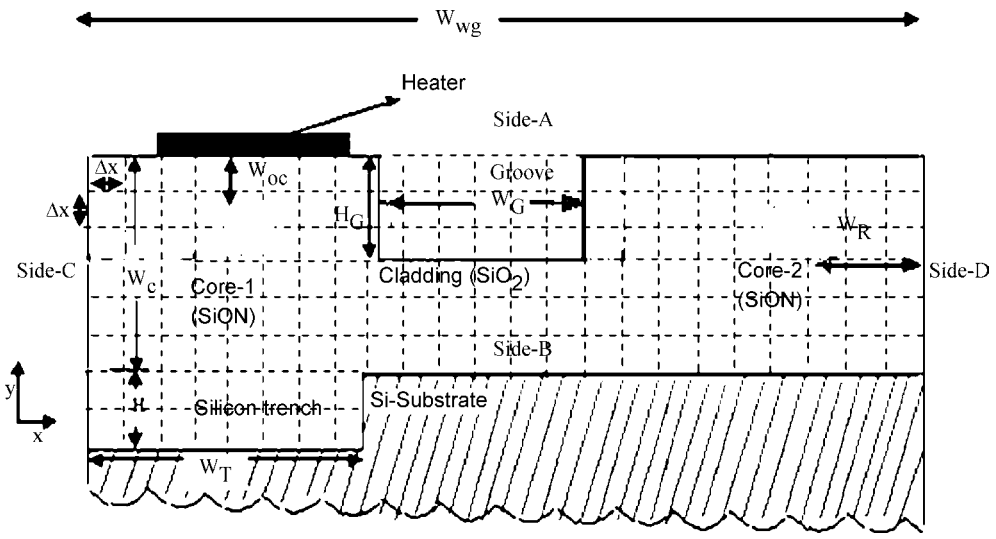

FIGURE 3 Cross sectional view of proposed thermooptic delay line structure consisting of single stress releasing grooves of depth H_G and width W_G, and silicon trench of trench height H_T and width W_T (cladding width $= W_c$, upper cladding width $= W_{oc}$, and device width $= W_{wg}$)

sion. The temperature gradient obtained from the temperature profiles by using implicit finite difference temperature equations [12] is an important factor for studying the stress release groove in which, higher is the magnitude of temperature gradients, more is the stress release.

These implicit temperature equations are obtained at discrete points. The first step in this method is to select these points. The waveguide medium for which the temperature distribution has to be obtained with application of heat flux of q_0 via a heater is divided into a number of small regions of the same width, same length and height of Δx assigned to each reference point that is at its center. This reference point is referred to as a nodal point or node. Two types of nodes: interior nodes, which are situated inside the thermooptic structure, and surface nodes/exterior nodes, which are situated on the surface or boundary of the thermooptic structure as shown in Fig. 3. For computation, it is necessary to express these equations of the nodes in short form which can be written as

$$a_{i,i}T_i^{p+1} + \Sigma a_{i,j}T_j^{p+1} = b_i\,, \tag{6}$$

where the superscript p represents the time t ($t = p\Delta t$, where $\Delta t = (\Delta x)^2/4\alpha$). The first subscript i of coefficients $a_{i,i}$ represents the equation number, and the second subscript i indicates the node number. Similarly, the first i of coefficients $a_{i,j}$ represents the equation number, and the second subscript j indicates the neighboring node number of the ith node. T_i^{p+1} and T_j^{p+1} are the temperatures of the ith node and its neighboring node j, respectively. The coefficients of the temperature equations for all interior and surface nodes can be obtained easily from implicit temperature equations [12] and are given below:

$a_{i,i} = 8$, For all interior nodes, silicon trench nodes and air exposed top surface nodes,
$= 1$, for side surface nodes (side C and D), bottom surface nodes attached to the substrate and stress releasing groove nodes
$= 3$, for heater exposed top surface nodes.

$a_{i,j} = -1$, For all interior nodes, side surface nodes ($j = i+1$ for side C and $j = i-1$ for side D), heater exposed to top surface nodes ($j = i+m$, m = total number of nodes in a row of the device) and air exposed top surface nodes ($j = i \pm 1$), silicon trench nodes and stress releasing groove nodes,
$= -2$, for air exposed top surface nodes ($j = i+m$) $= 0$, otherwise.

$b_i = 4T_i^p$, For all interior nodes,
$= 2T_i^p + q_0\Delta x/k$, for heater exposed top surface nodes,
$= 0$, for side surface nodes (side C and D).
$= T_\mathrm{I}$, for bottom surface nodes,
$= T_\alpha$, for stress releasing groove nodes,
$= 4T_i^p + 2\mathrm{Bi}T_\alpha$, for air exposed top surface node and stress releasing groove nodes.

$k =$ Thermal conductivity of waveguide medium.
Bi = Biot's number [12].

The values of parameters of the SiO_2/SiON waveguide considered for computation of temperature profiles are given in Table 1 [12]. After assigning the initial temperature of all nodes at room temperature, the heat flux, q_0 of the heater is set at a value and the old temperatures of all the nodes are updated with new temperatures by inserting $p = p+1$ till t is equal to the time needed to obtain the required temperature difference between the cores.

Parameters	Values
Thermal conductivity (K) of silica	$2.0\,\mathrm{W\,m^{-1}C^{-1}}$
Specific heat (C_p) of silica	$700\,\mathrm{J\,C^{-1}kg^{-3}}$
Specific gravity (ϱ) of silica	$3.5\times10^3\,\mathrm{kg\,m^{-3}}$
Heat convection coefficient (h) of air	$10\,\mathrm{W\,m^{-2}C^{-1}}$
Ambient temperature (T_α) of air	25 °C
Room temperature (T_I)	25 °C
Thermal diffusivity ($\alpha = k/\varrho C$)	$8.163\times10^{-7}\,\mathrm{m^2/s}$
Biot' s number ($\mathrm{Bi} = h\Delta x/k$)	15×10^{-6}

TABLE 1 Parameters used for determination of temperature profiles of the structures

The simulated results of temperature profiles (T vs. x) of conventional and proposed structures with the groove placed at a distance 2 μm from the heater in between two cores, obtained using (6) for different values of H_G (up to $x =$ 42 μm) are shown in Fig. 4a ($W_\mathrm{H} = 6$ μm, $L_\mathrm{H} = 472$ μm, $\Delta T_\mathrm{c} = 15$ °C, $W_\mathrm{c} = 15$ μm, core size $\sim 1.5\times1.5\,(\mu\mathrm{m})^2$ and $\Delta n = 5\%$). The separation between two cores (W_S) varied from 10 to 70 μm is considered for thermal analysis of the structure. In the figure, the temperatures of the profiles are taken in the plane passing through the cores at the middle of the delay line where W_G is taken to be 9 μm. It is seen that the temperatures near the groove decreases as H_G increases. In the case of the conventional structure, the temperature decreases slowly with increase of x near the groove. The absolute value of the temperature gradient near the grooves for the conventional structure ($H_\mathrm{T} = H_\mathrm{G} = 0$ μm) between two cores along the x direction is calculated as 0.69 °C/μm, whereas the curves near the groove (shown in the figure) between two cores in the proposed structure (trench height $H_\mathrm{T} = 9$ μm and trench width $W_\mathrm{T} = 18$ μm) with $H_\mathrm{G} = 0$, 6, 9 and 15 μm are estimated as 0.82, 3.56, 4.7, and 4.8 °C/μm, respectively. The absolute value of the temperature gradient of the conventional structure is lower than that of other structures. The value increases slightly due to the presence of the silicon trench just below the heater in the proposed structure without the groove, and increases with increase of groove depth, H_G and after a certain depth of stress releasing grooves ($H_\mathrm{G} \sim 9$ μm), the temperature gradients along the horizontal direction are almost saturated. The absolute value of the temperature gradient of the proposed structure with $H_\mathrm{G} = 9$ μm is ~ 9 times more than that of the conventional structure. At other portions of the delay line structure along the z-axis, the temperature profiles (T vs. x) for $W_\mathrm{H} = 6$ μm, $L_\mathrm{H} = 472$ μm, $\Delta T_\mathrm{c} = 15$ °C, $W_\mathrm{c} = 15$ μm, core size$\sim 1.5\times1.5\,(\mu\mathrm{m})^2$ and $\Delta n = 5\%$ are shown in Fig. 4b. It is seen from the figure that temperature profiles at 50 μm left of the middle of the delay line and 50 μm right of the middle of the delay line along z-axis are almost close with that at the middle of the delay line. Therefore, it is clear that an all through stress releasing groove is not required for the release of temperature induced stresses, which reduces polarization dependent losses as discussed in the next section.

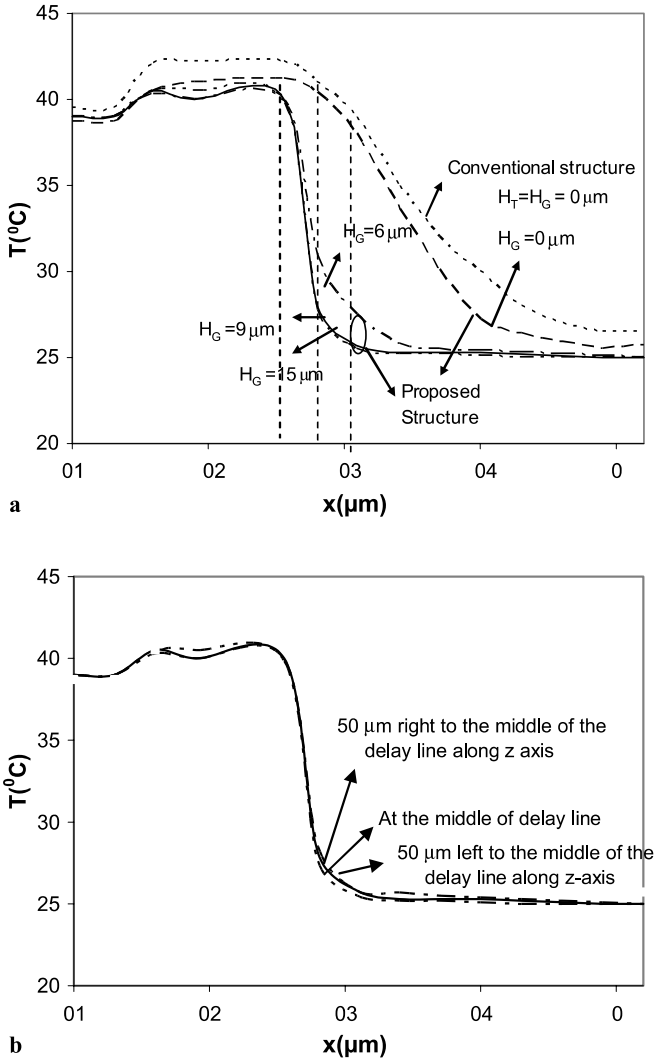

FIGURE 4 (**a**) Temperature provile (T vs. x) for the conventional structure ($H_G = H_T = 0\,\mu m$) and proposed structure with different values of H_G ($W_H = 12\,\mu m$, $L_H = 5\,mm$, $W_T = 18\,\mu m$, $H_T = 12\,\mu m$, $W_c = 15\,\mu m$, $\Delta T_c = 15\,^\circ C$, $\Delta n = 5\%$ and $W_{wg} = 42\,\mu m$). (**b**) Temperature profile (T vs. x) for the proposed structure ($H_g = 9\,\mu m$) at the middle of the delay line, 50 μm left of the middle of the delay line and 50 μm right of the middle of the delay line along the z-axis ($W_H = 12\,\mu m$, $L_H = 472\,\mu m$, $W_T = 18\,\mu m$, $H_T = 12\,\mu m$, $W_c = 15\,\mu m$, $\Delta T_c = 15\,^\circ C$, $\Delta n = 5\%$)

4 Polarization independent transmission characteristics

Figure 5 shows simulation results of the normalized cross state transmission characteristics of TE and TM polarization obtained by using (1)–(4) for a five-stage Y symmetric CMZ filter based on the proposed structure having a groove depth of $H_G = 9\,\mu m$ with $W_H = 6\,\mu m$, $L_H = 472\,\mu m$, $W_c = 15\,\mu m$, core size $\sim 1.5 \times 1.5\,(\mu m)^2$, $\lambda_{ref} = 1.55\,\mu m$, cladding index = 1.447 and $\Delta n = 5\%$. In Fig. 5 the difference between transmission characteristics of TE and TM polarization for the proposed structure having a groove is small in comparison to the conventional structure having no groove (shown in Fig. 2). The shift of resonant wavelength due to heating the curved arm of the delay line section by the heater is the same in both TE and TM polarization, because anisotropic stress developed due to the temperature difference

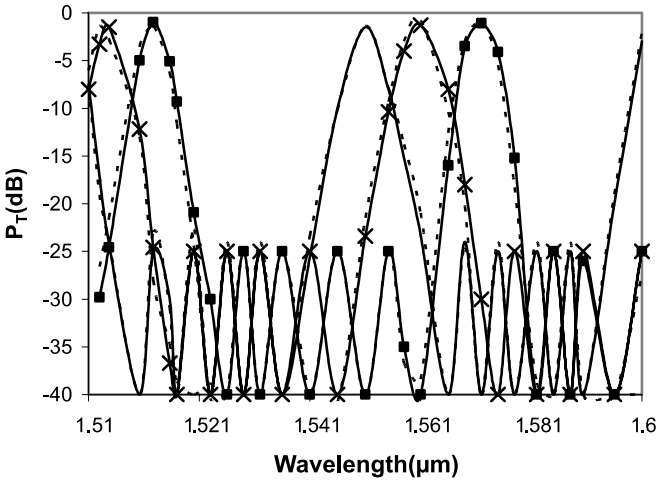

FIGURE 5 Polarization independent tunable transmission characteristics of a five-stage Y symmetric CMZ filter based on the proposed thermooptic delay line structure with $\Delta n = 5\%$, $\lambda_{ref} = 1.55\,\mu m$, cladding index = 1.447, waveguide core width $w = 1.5\,\mu m$, $\Delta L = 20.5\,\mu m$ and $L_B = 462\,\mu m$

between two cores (causing an extra phase difference in TM polarization) is released by the groove. The PDL of the device estimated from the figure by using (5) for $\Delta T_c(P)$ of 6 and 12 °C are ~ 0.08 and ~ 0.081 dB, respectively. Due to the presence of a stress releasing groove in the proposed thermooptic delay line structure, the PDL remains almost constant with an increase of temperature and the PDL is almost negligible in comparison to the conventional structure as shown in Fig. 2. Therefore, polarization dependence of transmission characteristics in the proposed structure is smaller than that of the structure having no groove. In Fig. 5, the reduction of the peak normalized cross state power is mainly due to bending loss, which is approximately 0.1 dB per MZ section. The heating power (H) required per delay line section to achieve $\Delta T_c(P)$ of 6 and 12 °C for the tuning of an add/drop multiplexer based on CMZ coupler with conventional structure to wavelength 1.56 and 1.57 μm from 1.55 μm is estimated by using the equation $H = q_0 W_H L_H$ (where, q_0 = heat flux required to achieve these temperature differences, W_H = heater width and L_H = heater length) as 84.2 and 178 mW per delay line section, respectively. For the proposed structure to tune to the same wavelengths, the heating power required is 53 and 108.4 mW, respectively. Therefore, the reduction of the heating power in the proposed structure is ~ 1.6 times less that of the conventional structure.

5 Conclusion

In this paper, it is found that an add/drop multiplexer based on a Y symmetric cascaded Mach–Zehnder (CMZ) coupler is polarization dependent due to the stress anisotropy caused by local heating for thermal tuning. A thermooptic delay line structure with stress releasing groove is proposed for the reduction of polarization dependent characteristics of a high index contrast Y symmetric delay line structure of the device. It is seen from thermal analysis that the absolute value of the temperature gradient of the proposed structure which mainly causes the release of stress anisotropy is ~ 9 times more than that of the con-

ventional structure. It is also seen that the polarization dependent loss of thermally tunable transmission characteristics of the *Y* symmetric CMZ device based on the structure proposed here is 0.08 dB, which is negligible in comparison to that based on the conventional structure. Further, it is found that the heating power required for tuning of the add/drop multiplexing by the proposed structure is reduced by a factor of 1.6 compared to that of the conventional structure.

REFERENCES

1 H.H. Yaffe, C.H. Henry, M.R. Serbin, L.G. Cohen, IEEE J. Lightwave Technol. **12**, 10 (1994)
2 C. Kostrzewa, R. Moosburger, G. Fisehbech, B. Schuppert, K. Petermann, IEEE Photon. Technol. Lett. **9**, 1487 (1997)
3 M. Kuznetsov, IEEE J. Lightwave Technol. **12**, 225 (1994)
4 C. Kostrzewa, R. Moosburger, G. Fisehbech, B. Schuppert, K. Petermann, IEEE Photon. Technol. Lett. **7**, 902 (1995)
5 M. Sharma, H. Ibe, T. Ozeki, IEEE J. Lightwave Technol. **15**, 917 (1997)
6 P.P. Sahu, A.K. Das, Proc. Comnam, Kolkata, 47, December, (2000)
7 L. Dong, P. Hua, T.A. Birsk, L. Reekie, P.S.J. Russel, IEEE Photon. Technol. Lett. **8**, 1656 (1996)
8 G.P. Agrawal, S. Radic, IEEE Photon. Technol. Lett. **6**, 995 (1994)
9 H. Venghaus, Appl. Phys. Lett. **61**, 2018 (1992)
10 P.P. Sahu, Fiber Integ. Opt. **27**, 24 (2008)
11 A. Sugita, K. Jinguji, N. Takato, K. Katoh, M. Kawachi, Trans. Electron. IEICE **E73-E**, 105 (1990)
12 A.K. Das, P.P. Sahu, J. Opt. **32**, 151 (2003)
13 Y. Inoue, K. Katoh, M. Kawachi, IEEE Photon. Technol. Lett. **4**, 36 (1992)
14 B.J. Offrein, D. Jubin, T. Koseter, T. Brunschwiler, F. Horst, D. Wiesmann, I. Meijer, M. Sousa Petit, D. Webb, R. Germann, G.L. Bona, IEEE Photon. Technol. Lett. **16**, 1483 (2004)
15 Y. Hida, N. Takato, K. Jinguji, IEE Electron. Lett. **31**, 1377 (1995)
16 P.P. Sahu, Appl. Opt. **47**, 718 (2008)
17 A.K. Das, P.P. Sahu, IEEE Wireless Opt. Commun. Conf. 01 666 673, 1–5 (2006)
18 P.P. Sahu, Indian J. Phys. **82**, 137 (2008)
19 H. Nishihara, M. Haruna, T. Suhara, *Optical Intagrated Circuits* (McGraw-Hill, New York, 1989)